J. Chem. Eng. Data 1990, 35, 125-127

Solubility and Mass-Transfer Coefficients for Hydrogen and Carbon Monoxide in *n*-Octacosane

Sarah A. Miller* and Alf Ekstrom

CSIRO Division of Fuel Technology, Lucas Heights Research Laboratories, Menai, NSW 2234, Australia

Neil R. Foster

School of Industrial Chemistry and Chemical Engineering, University of New South Wales, Kensington, NSW 2033, Australia

The solubility and mass-transfer coefficients for hydrogen and carbon monoxide have been determined in a Fischer–Tropsch slurry with use of a modified continuously stirred tank reactor. Experiments were performed at 528 K and 1–3 MPa in *n*-octacosane. The solubility coefficients were found to be similar to those reported for industrial waxes. The presence of solids does not affect the solubilities. The effect of stirrer speed on the mass-transfer coefficients was found to be significant between 250 and 1750 rpm.

Introduction

The kinetics of Fischer–Tropsch synthesis in slurry bubble column reactors approaches the regime of being either mass transfer or chemically controlled. To be able to satisfactorily model a bubble column under Fischer–Tropsch conditions, the mass-transfer and solubility coefficients for each of the reacting gases and their chemical reaction rates need to be determined. The slurry is composed of both wax and catalyst, and the mass-transfer kinetics may be affected by the presence of the catalyst. Consequently, it was decided that the mass-transfer and solubility coefficients for hydrogen and carbon monoxide should be determined in a slurry on *n*-octacosane and an iron-based catalyst.

Experimental Section

The method reported by Ledakowicz (*1*) has been used to determine the gas–liquid mass-transfer coefficients in the spent slurry. The experimental setup showing details of the autoclave and impellor is shown in Figure 1. The 0.31 autoclave (Autoclave Engineers 300cc packless autoclave assembly Model 316SS) was fitted with an electrically driven belt and a magnetic stirrer. The preheated gas was fed in through the head of the reactor, above the slurry. A pressure transducer was also attached to the head. Two thermocouples were placed inside a thermowell to measure both the gas- and liquid-phase temperatures. The pressure transducer and thermocouples were connected to a data taker controlled by a microcomputer.

The slurry was heated to 523–528 K and, upon attainment of thermal equilibrium, was degassed with a vacuum pump. Hydrogen or carbon monoxide was used to pressurize the autoclave to approximately 1, 2, or 3 MPa and the data collection started. The stirrer was then engaged until the pressure stabilized. A typical experimental profile of pressure versus time is shown in Figure 2. The volumetric mass-transfer coefficient was calculated from

$$dN_{gas}/dt = V_{liquid}k_{L}a(C_{L,1} - C_{L,2}) \qquad (1)$$

The solubility of the gas was calculated from Henry's law

$$C_{L} = P_{eq}/H \qquad (2)$$

where the liquid-phase concentration was calculated from

$$C_{L} = \frac{V_{gas}}{V_{liquid}} \frac{(P_{0} - P_{eq})}{RT} \qquad (3)$$

Table I. Summary of Mass-Transfer Coefficients for Hydrogen and Carbon Monoxide at Various Stirrer Speeds and Initial Pressures[a]

gas	stirrer, rpm	temp, K	k_La, s^{-1}	P_0, MPa	P_{eq}, MPa	C_L, mol/L
H_2	250	525	0.02	2.19	2.03	0.081
H_2	750	525	0.09	2.19	2.01	0.091
H_2	1250	526	0.97	1.52	1.40	0.063
H_2	1250	526	0.93	2.13	1.95	0.091
H_2	1250	528	0.94	3.05	2.80	0.129
H_2	1750	526	1.28	2.20	2.02	0.088
CO	250	526	0.04	2.21	2.05	0.081
CO	750	525	0.09	2.21	2.00	0.106
CO	1000	525	0.41	2.18	1.98	0.101
CO	1250	526	0.83	1.15	1.04	0.053
CO	1250	526	0.95	2.08	1.88	0.101
CO	1250	528	1.08	3.20	2.90	0.151
CO	1750	525	1.50	2.18	1.98	0.101

[a] The equilibrium pressures and concentrations of material dissolved in the liquid phase are also given.

Table II. Solubility Coefficients (MPa L mol^{-1}) for Hydrogen and Carbon Monoxide

ref	H_2	CO	wax	temp, K
this work	19.16	21.74	nC_{28}	528
2	22.20	19.60	Gulf	523
3	29.20	21.60	FT-heavy	523
4	27.30	23.07	Mobil FT	543

Results and Discussion

Table I summarizes the solubility and mass-transfer data collected. Figure 3 shows the liquid-phase concentrations plotted against the equilibrium pressure for both hydrogen and carbon monoxide. The linearity shows that Henry's law is obeyed in both cases. The solubility coefficients, for this work and work reported elsewhere, are listed in Table II.

The values determined in this work compare favorably with the values reported by Albal et al. (*2*). The wax used by Albal et al. has a hydrocarbon distribution centered around the octacosane. The hydrogen solubility reported by Karandikar (*3*) is higher than expected, as were other hydrogen solubilities determined by Karandikar in the heavy Fischer–Tropsch was at different temperatures. Huang et al. (*4*) also reported higher solubilities for both carbon monoxide and hydrogen in a Fischer–Tropsch wax from the Mobil bubble column pilot plant. This work was done at a slightly higher temperature.

The equivalence between the solubilities in the industrial waxes (Table I) and the pure *n*-octacosane wax demonstrates that studies of the Fischer–Tropsch reaction in the pure wax will be analogous to the industrial wax. This is particularly relevant for quantifying the distributions of the Fischer–Tropsch hydrocarbon products.

The presence of solids in the wax may have affected the physical properties, such as the viscosity, of the *n*-octacosane, which in turn may have affected the gas solubilities. The similarity in solubilities of both hydrogen and carbon monoxide in

0021-9568/90/1735-0125$02.50/0

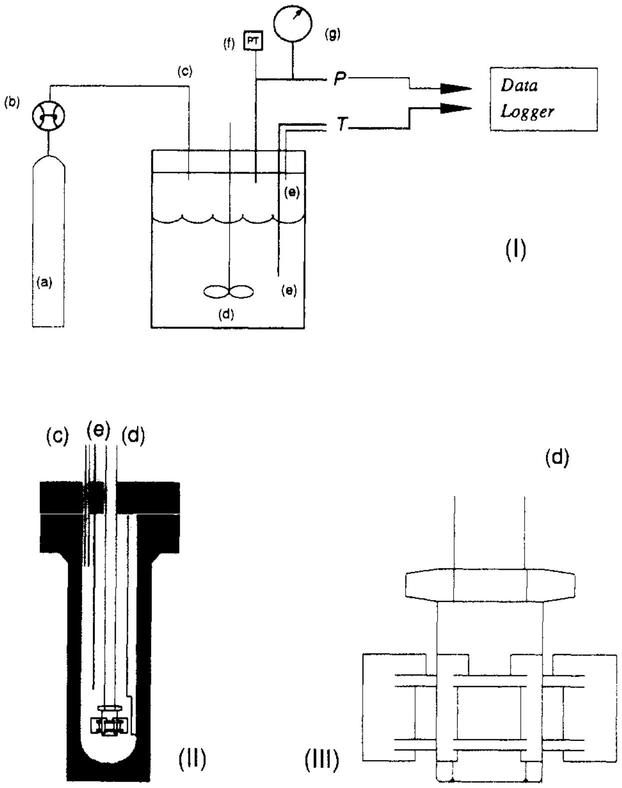

Figure 1. Experimental setup (I) showing details of the autoclave (II, 46-mm i.d., 180-mm depth) and impellor (III, 6 blades, 31.7-mm o.d.): (a) gas supply; (b) pressure regular; (c) inlet gas line; (d) impellor; (e) thermocouple well; (f) pressure tranducer; (g) pressure guage. (P = pressure signal, T = temperature signal).

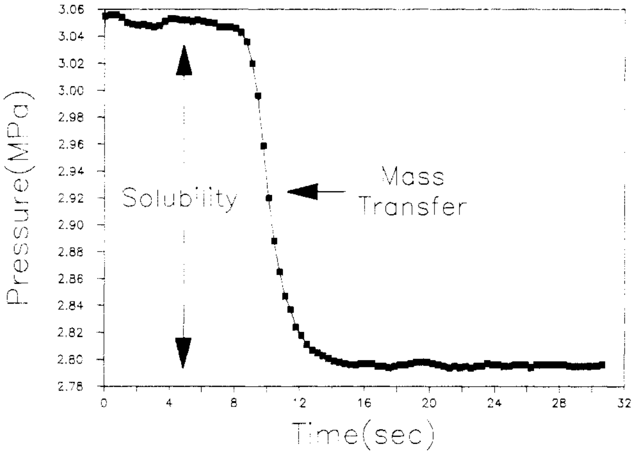

Figure 2. Typical experiment profile of pressure versus time. The pressure drop is related to the solubility, and the rate of the pressure drop is related to the mass-transfer rate.

this work and the reported work (Table II) indicates that the presence of the catalyst does not affect the solubility of these gases.

Table I lists the mass-transfer coefficients for hydrogen and carbon monoxide at various stirrer speeds and pressures. Figure 4 shows that the stirrer speed has a dramatic effect on the rate of mass transfer of both hydrogen and carbon monoxide. Ledakowiscz et al. (*1*) and Karandikar et al. (*5*, *6*) have seen similar effects and compared them in terms of specific power input. This result is particularly significant for modeling and running reactors, such as bubble column reactors, where there is no mechanical stirring. In a bubble column reactor, the degree of mixing is dependent upon the motion of the gas bubbles and this result suggests that the rate of mass transfer is also dependent upon the gas bubble motion.

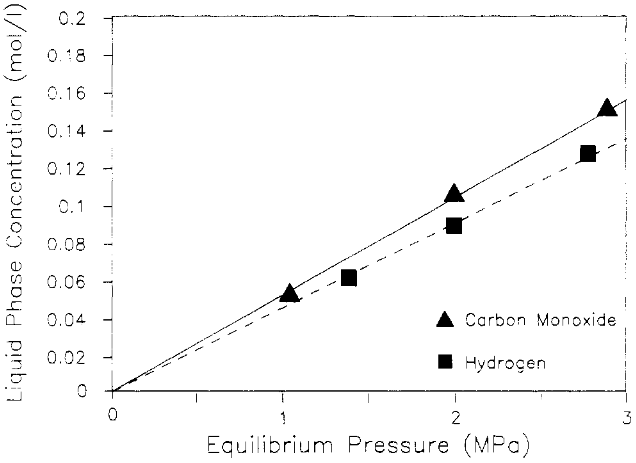

Figure 3. Graph showing Henry's law: the direct dependence between liquid-phase concentration and equilibrium pressure.

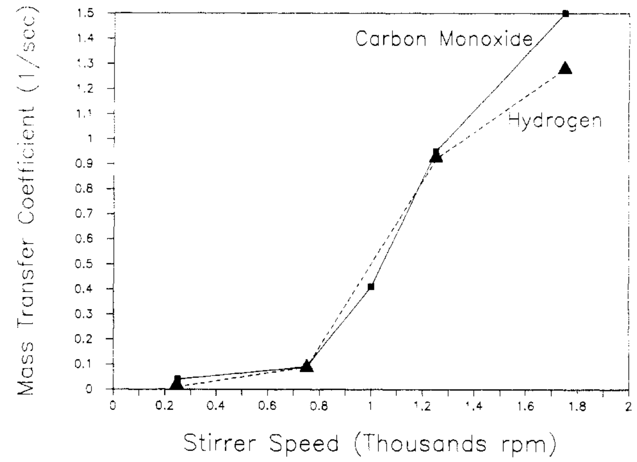

Figure 4. Effect of stirrer speed on mass-transfer coefficient.

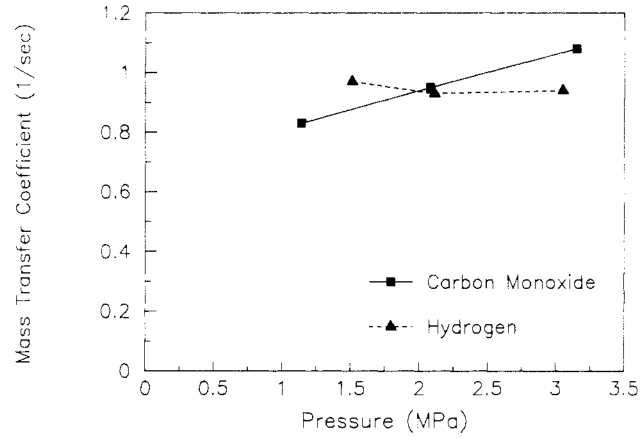

Figure 5. Effect of pressure on mass-transfer coefficients.

It has come to the attention of two of the authors (*7*), that Fischer–Tropsch synthesis in a bubble column reactor can drop dramatically over a small change in linear velocity, at low linear velocities (1 cm s^{-1}). This loss of activity is assumed to be due to mass-transfer resistances since slurry sampling showed no evidence of catalyst settling. Similar losses in activity were observed by Kuo (*8*) but were attributed to catalyst settling.

Pressure, in comparison, does not have a significant effect on the rate of mass transfer of either hydrogen or carbon monoxide. Figure 5 does suggest a slight variation in mass transfer with pressure, but given the large change in mass transfer with stirrer speed around 1250 rpm, this variation is not significant.

J. Chem. Eng. Data **1990**, *35*, 127–130

Acknowledgment

We thank Jan Chipperfield for her assistance in collecting the data.

Glossary

$C_{L,l}$	liquid-phase concentration (at time l) (mol L^{-1})
H	solubility coefficients (MPa L mol^{-1})
k_La	mass-transfer coefficient (s^{-1})
N	number of moles (mol)
P	pressure (MPa)
R	gas constant
t	time (s)
T	temperature (K)

Subscripts

V	volume (L)
0	time = 0
eq	equilibrium

Registry No. H_2, 1333-74-0; CO, 630-08-0; *n*-octacosane, 630-02-4.

Literature Cited

(1) Ledakowiscz, S.; Nettlehof, H.; Deckwer, W.-D. *Ind. Eng. Chem. Fundam.* **1984**, *23*, 510.
(2) Albal, R. S.; Shah, Y. T.; Carr, N. L.; Bell, A. T. *Chem. Eng. Sci.* **1984**, *39*, 905.
(3) Karandikar, B. M. An experimental study of gas liquid mass transfer at Fischer-Tropsch reaction conditions. Ph.D. Thesis, University of Pittsburgh, 1986.
(4) Huang, S. H.; Lin, H. M.; Tsai, F. N.; Chao, K. C. *Ind. Eng. Chem. Res.* **1988**, *27*, 162.
(5) Karandikar, B. M.; Morsi, B. I.; Shah, Y. T.; Carr, N. L. *Chem. Eng. J.* **1986**, *33*, 157.
(6) Karandikar, B. M.; Morsi, B. I.; Shah, Y. T.; Carr, N. L. *Can. J. Chem. Eng.* **1987**, *65*, 973.
(7) Miller, S. A.; Ekstrom, A. Unpublished work.
(8) Kuo, J. C. W. Slurry Fischer-Tropsch/Mobil two stage process of converting syngas to high octane gasoline. Final Report, DOE/PC/30022-10, 1983.

Received for review February 28, 1989. Accepted December 6, 1989. This work was supported by a CSIRO/UNSW Collaborative Research Fund.

Viscosity Behavior of Potassium Iodide in *N*-Formylmorpholine Solutions at Several Temperatures

Souad F. Al-Azzawi* and Muna A. Salman

Petroleum Research Centre, Jadiriyah, P.O. Box 10039, Baghdad, Iraq

The viscosity of potassium iodide in *N*-formylmorpholine was measured at 25, 35, 45, and 55 °C in a range of 0–1.0 M composition. The viscosity shows a negative deviation over the whole composition range and all the temperatures studied. The activation energies of viscous flow were calculated, and their significance is discussed. The ionic *B* coefficients have been determined at low concentrations and interpreted qualitatively.

Introduction

Ion–solvent interactions have been studied extensively in aqueous solution (*1–4*). Less attention has been given to such interactions in nonaqueous solvents. Therefore, we have initiated a program to study ion–solvent interactions of salts in highly dense, highly polar, and highly selective solvents for the extraction of monocyclic aromatic hydrocarbons, such as *N*-formylmorpholine (*5*), ethylene glycol (*6*), and *N*-methylpyrrolidone (*7*). These solvents readily dissolve potassium iodide. As a first part of this work, we have measured the densities and viscosities of potassium iodide in *N*-formylmorpholine in the range of 0–1.0 M and at 25, 35, 45, and 55 °C. The Jones and Dole (*8*) empirical equation has been used for determining viscosity *B* coefficients at low concentrations.

Experimental Section

Materials. *N*-Formylmorpholine (NFM), Puriss Grade (Fluka AG), was used without further purification, kept over an activated molecular sieve of type 4A (Union Carbide) for 2 days, and filtered before use. The purity was checked by GLC and was found to be >99.5 mol %.

Potassium iodide (KI), Chemically Pure (Riedel-de Haen AG), was dried for 24 h at 110 °C prior to use and stored over P_2O_5 in a glass desiccator.

Densities Measurements. Densities were determined with an Anton Paar (Model DMA 602) digital densimeter, thermostated to ±0.01 °C. The overall precision of the densities is estimated to be better than $\pm 2 \times 10^{-6}$ g cm^{-3} for 25, 35, and 45 °C and $\pm 4 \times 10^{-5}$ g cm^{-3} for 55 °C.

Viscosity Measurements. Viscosities were determined with a suspended-level Ubbelohde viscometer. The flow times were determined electronically with an electronic timer of precision ±0.01 s, and the temperature of the bath was controlled to be better than ±0.01 °C. Viscosities of all solutions were reproducible within ±0.5% at all temperatures studied.

Preparation of Salt Solutions. Solutions were made up by weight with use of a four-place digital balance. Stock solutions of the KI in NFM were prepared by direct weighing, and these were diluted accurately by using previously calibrated glassware to obtain different required concentrations.

Results and Discussion

The obtained densities, viscosities, and refractive indices of solutions of KI in NFM at 25, 35, 45, and 55 °C are listed in Table I. The viscosity increases with decreasing temperature and with increasing molar concentration of KI, Figure 1.

The experimental data were analyzed for low molar concentrations of KI in NFM according to the Jones–Dole equation (*8*)

$$(\eta/\eta_0 - 1)/C^{1/2} = A + BC^{1/2} \qquad (1)$$

where η and η_0 are the viscosities of the solution and pure solvent, respectively; *A* and *B* are the characteristic parameters for salt and solvent, dependent on ion–ion and ion–solvent interactions, respectively; and *C* is the molar concentration of KI in NFM. Plotting $(\eta/\eta_0 - 1)/C^{1/2}$ against $C^{1/2}$ at 25, 35, 45, and 55 °C yields an exponentially increasing function, Figure 2a–d.

0021-9568/90/1735-0127$02.50/0 © 1990 American Chemical Society